Optically Upconverted, Spatially Coherent Phased-Array-Antenna Feed Networks for Beam-Space MIMO in 5G Cellular Communications

[a,b]Dennis Prather, [b]Connor Creavin, [b]Timothy Creazzo, [b]Charles Harrity, [b]Janusz Murakowski, [a,b]Xiao-Feng Qi, [a,b]Garrett Schneider, [b]Christopher Schuetz, [a,b]Shouyuan Shi, [b]Kevin Shreve, [b]Fuquan Wang, and [b]Peng Yao

[a]University of Delaware, Electrical and Computer Engineering, 139 The Green, Newark, Delaware, DE, USA 19716
[b]Phase Sensitive Innovations, Inc., 116 Sandy Drive, Newark, DE, USA 19713

Abstract: We present an RF-photonic phased-array receiver that provides simultaneous multi-band and multi-beam operation in the millimeter-wave region of the spectrum. It uses a photonic integrated circuit to perform RF beamforming with near unlimited beam-bandwidth product.

1. Introduction

The presented phased array system offers spectral agility and spatial diversity with low size, weight, and power (SWaP). This work is motivated by the rapid expansion of 5G and B5G technologies, where millimeter waves (mmW) have been incorporated into the latest 5G standard with FR2 (frequency range 2) bands spanning 24.25—52.6 GHz with bandwidths up to 400 MHz for both up-link and down-link. 3GPP Release 17 expands the spectral range up to 71 GHz to support the global 60 GHz unlicensed band with bandwidths up to 2 GHz for integrated-access-and-backhaul (IAB). Furthermore, coverage enhancement via analog beamforming is being actively explored for Release 18 (a.k.a. 5G Advanced).

According to Friis equation, the use of higher electromagnetic frequencies comes with an associated increase in free-space path loss (FSPL), the mitigation of which requires a commensurate increase in antenna gain. However, high-gain antennas suffer from a decrease in spatial coverage that, in turn, necessitates the use of an array antenna to provide both high gain and wide spatial coverage without moving parts. The challenge then becomes that of a dense beam-space, which imparts significant performance requirements on the phased array systems ability to transmit or receive multiple broadband beams simultaneously. This challenge is expressed in a single figure of merit, the so-called beam-bandwidth product (BBP), which measures the total communication capacity of a phased array system.

To address these challenges, we developed a new phased array receiver (RX) system, shown in Fig. 1, where (a) illustrates the concept of optical up-conversion of received RF signals onto optical side bands directly at each element within the antenna array. The up-converted output of each antenna element is routed through an optical fiber to a bundle where it is re-launched into free space and overlaps with the output of every other fiber. Because the up-conversion process preserves the RF waveform, the amplitude and phase of the captured RF signal becomes the amplitude and phase of the re-launched optical signal from its corresponding fiber in the bundle. Consequently, the formed optical beams are exact replicas of all incident RF wavefronts. An optical lens placed after the bundle produces the two-dimensional spatial Fourier transform of the optical wavefront and, as such, focuses the resulting beams onto corresponding lens-coupled fibers, see Fig. 1(b). In doing so, each spatial sector is decoupled from, or rendered spatially orthogonal to, every other spatial sector thereby enabling independent operation of each sector. To realize this functionality, each focused beam is routed to a photodetector and mixed with an appropriately tuned optical local oscillator (TOLO) to produce an intermediate frequency (IF). A key point is that while an RF frequency is received on the input side, every output signal is at an IF frequency. As a result, there are no high-frequency RF devices, components, cables, or waveguides in the entire antenna system—except for the RF front end. Moreover, lower-sampling-rate analog-to-digital-converters (ADCs) can be used at IF to yield higher effective-number-of-bits (ENOB) and consume less power as compared to higher-sampling-rate ADCs. Finally, each signal is digitized and fed to a digital signal processor (DSP) for processing specific to a designated spatial channel.

Multiple one-dimensional prototype versions of this system have been built and demonstrated, see Fig. 2(a)-(b). Comprehensive characterization of the phased array system was performed using a 1×16 array that operated from 20 GHz to 40 GHz. Results of these experiments showed a noise figure (NF) of the system on the order of 7 dB at 23 GHz relative to an ideal beamformer of equivalent antenna gain. Isolation between spatial sectors was greater than 24 dB, by virtue of spatial orthogonality in the beams formed by the optical processor. The linear dynamic range was measured to be 140 dB-Hz and the spur-free dynamic range (SFDR), measured using two-tone intermodulation, was 100 dB-Hz$^{2/3}$ when both of the sources were located in the same spatial sector (in-beam, worst case). Additionally, the ability to form the full set of orthogonal beams simultaneously was demonstrated, as illustrated in Fig. 2 using a 1×7 array. It should be noted that a similar implementation where the system is operated in reverse mode is being developed for a transmit (TX) phased array system.

2. Experimental Results

The demonstration experiments illustrated below show the capability of the imaging-receiver (IMRX) technology. However, it should be noted that the quantitative results presented here do not represent its performance limits, but instead are constrained by the limitations of the available signal generation sources. The two experiments highlight several key unique features:

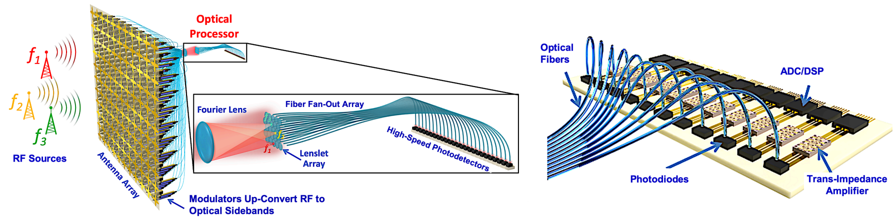

(a) (b)

Figure 1. An RF-Photonic phased-array system that "images" incident RF signals into independent spatial sectors in a lenslet array wherein each lenslet corresponds to a unique detector that, in turn, corresponds to a unique resolved beam for signal recovery. (a) Conceptual overview. (b) Detailed illustration of the back-end pickup fibers and photodetection hardware.

- Analog optical beamforming: ALL beams accessible to the array, based on its aperture size and element count, are formed simultaneously and continuously using an optical lens, with speed of light latency and zero power consumption.
- Virtually unlimited beamforming bandwidth: The entire RF spectrum is narrow compared to optical-frequency carriers, so the optical beamforming operation is RF-carrier-frequency agnostic and can process extremely wide IBW signals with negligible dispersion.
- High-fidelity IF waveform recovery: Using a widely tunable optical LO after beamforming allows RF waveforms to be down-converted to any desired IF, enabling the use of photodiodes and ADCs optimized for the IBW rather than the RF carrier, thereby increasing fidelity and dynamic range and reducing component cost.

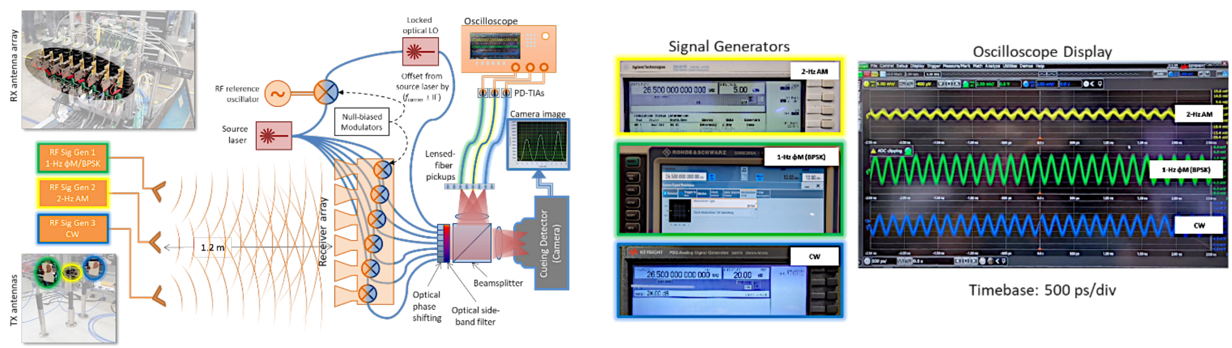

(a) (b)

Figure 2. (a) BBP experiment schematic showing three TX antennas illuminating the IMRX system. (b) Photos of the signal generators' panels showing the exact same TX frequency, with insets indicating the modulation conditions used, and of the IMRX output waveforms at 5-GHz IF.

2.1 Beam-Bandwidth Product (BBP) 15 GHz

The system's capacity to form beams for UWB signals on high-frequency RF carriers is virtually unlimited. In Fig. 2, the prototype used 7 elements, and hence 7 accessible beams, to demonstrate this capacity experimentally. The results are shown in Fig. 2(b) where three signal generators were set up, each transmitting at the same frequency of 26.5 GHz. The system receives all the signals by optical up-conversion, beamforms in the optical domain to spatially separate the signals, then overlays them with an optical LO offset from the upconverted signals by an IF that can be anywhere from 1 MHz to 5 GHz. The mixing of the upconverted signals with the LO on photodiodes produces IF output signals that are displayed on an oscilloscope. The image of the scope display in Fig. 2(b) is actually a single frame from a video capture; in the video, the three TX sources are readily distinguished by their modulations: AM (yellow trace), PM (green), or none/CW (blue). These measurements confirmed that the three captured signals are separated according to the 3 distinct TX antenna positions. An IF of 5 GHz, multiplied by 3 occupied beams, demonstrates 15 GHz BBP capacity. Note however, that the system forms 7 beams simultaneously and could demonstrate all beams, were more signal generators available. Further, the IF upper limit of ~5 GHz is due to the output photodiode-transimpedance amplifier (PDTIA) devices used; similar devices are commercially available with ~10 GHz bandwidth, and standalone high-speed PDs can provide even greater IF bandwidth. Hence, the demonstrated 15 GHz is far less than the true capacity of this, relatively modest, system.

2.2 Aggregate Data Throughput 6 Gbps

To demonstrate the fidelity of the IF output signals, we used an experiment very similar to the one just described where two TX sources were set up, both at the same carrier frequency of 27.5 GHz. Because only two vector signal generators were available, this experiment used two TX sources rather than three. These signals were modulated with PRBS data in two different complex modulation formats: 16-QAM and 16-APSK, each encoding 4 bits per symbol. Due to the signal generators' baseband modulators' BW limitations, the symbol rates were 1.2 GHz and 300 MHz, respectively, corresponding to data rates of 4.8 Gbps and 1.2 Gbps. Hence, the total data rate was 6 Gbps. The two sources' upconverted signals were beamformed optically and detected by separate PDTIAs using the optical LO tuned for a 2-GHz IF center frequency. The IF waveforms were demodulated using a signal analyzer with vector signal analyzer software. Demodulated signal constellations are shown in Fig. 3 in tabulated format, where the columns correspond to conditions where either one TX source or the other was transmitting, or both simultaneously. The top and middle rows show the demodulator outputs for each condition. The bottom row contains line-scan camera images of the two sources indicating how they are spatially resolved. The center column depicts the demodulated data that was recovered with both sources transmitting independent data simultaneously at the same carrier frequency, with minimal SNR degradation, demonstrating the IMRX's ability to mitigate co-channel interference.

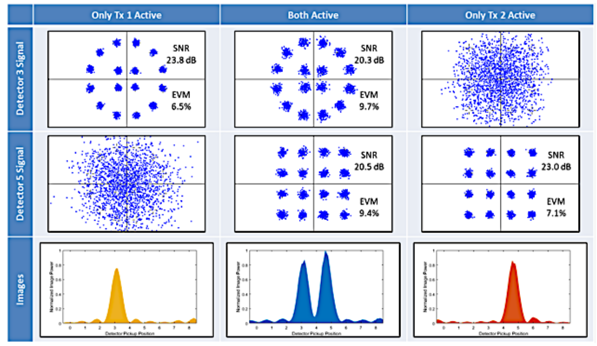

Figure 3. Experimental results from the IMRX when used to capture and beamform signals from two sources simultaneously, with the same carrier frequency and independent complex data modulation.

3. Photonic Integrated Circuit Beamformer

To achieve a smaller SWaP-C, we developed a photonic-integrated-circuit (PIC) implementation of the system, shown in Fig. 4. After up-conversion at the front-end, instead of relaunching into free-space, the optical signals are coupled onto a PIC using a standard fiber v-groove array (VGA). The beamforming on the PIC is accomplished using a star coupler. The outputs of the star coupler are coupled off the chip using another VGA, and that array of fibers is subsequently imaged onto a camera to allow us to effectively see the output of the PIC, see Fig. 4(b) and (c). After calibration, we were able to confirm the beamforming capability of the PIC by imaging the output of the PIC onto an IR camera and observing a single output that corresponds to the phase profile of the incoming optical signals to the PIC. Furthermore, we verified that the spot moves to different output locations by changing the phase profile of the incoming optical signals. These results are illustrated in Fig. 4 (b) and (c), which shows the IR images of the PIC output for two different phase profiles. Each phase profile results in the light getting routed to a different output of the PIC. In this integrated PIC implementation, an RF signal arriving at the phased array antenna will impose a phase profile across the antenna elements that will be preserved by the lithium niobate modulator array during up-conversion. As such, the optical signals on the PIC will be a copy in amplitude and phase of any incoming RF signal, and after beamforming (Fourier transform) the incoming angle of arrival will be mapped to a physical location at the output of the PIC.

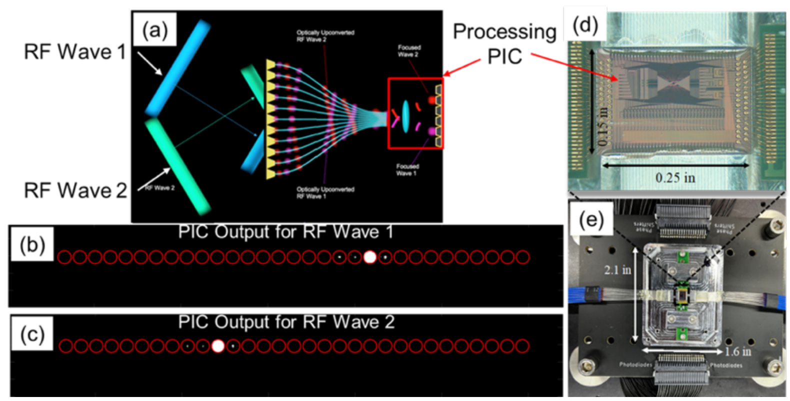

Figure 4. (a) Schematic image illustrating the correspondence between beamformed output and input phase profile; (b) PIC output imaged on an IR camera for phase profile 1; (c) PIC output imaged on an IR camera for phase profile 2; (d and e) Pictures of the packaged PIC.

4. Conclusion

In this work, we demonstrated a new class of RF phased array systems that performs beamforming with a nearly unlimited beam-bandwidth product. The beamforming also requires only minimal (<100 W) DC power and has a latency that is only limited by the speed of light, regardless of the IBW and the number of beams being processed. Such a capability is key to future 5G and B5G wireless communication systems.